

Supplementary Information

Influence of Silver Grain Size, Roughness, and Profile on the Extraordinary Fluorescence Enhancement Capabilities of Grating Coupled Surface Plasmon Resonance

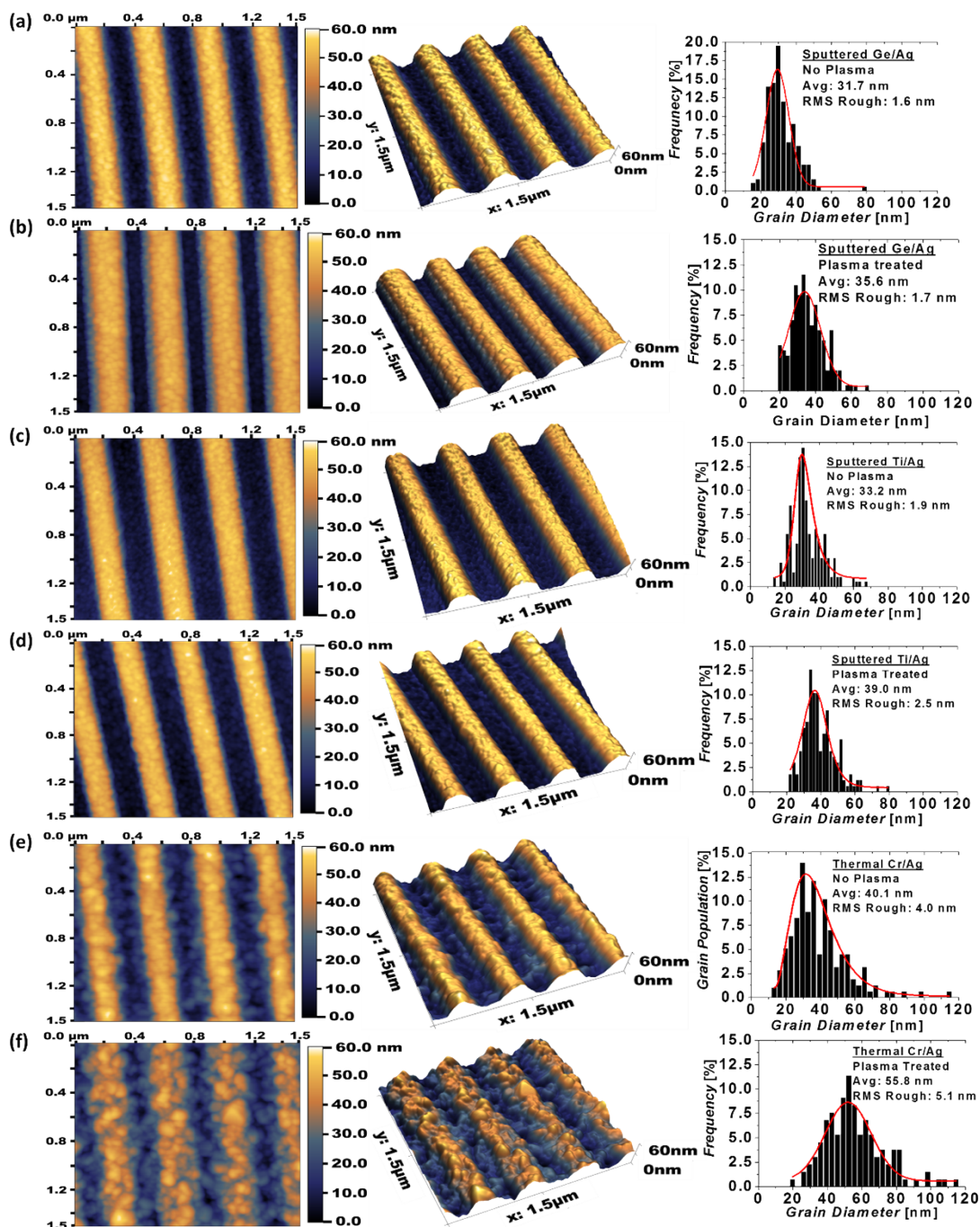


Fig. S1 2D and 3D Topographical AFM scans (1.5 $\mu\text{m} \times 1.5 \mu\text{m}$) and grain size distributions of gratings with (a,b) sputtered germanium and silver, (c,d) sputtered titanium and silver, and (e,f) thermally evaporated chromium and silver. Non-plasma treated samples (a,c,e) on average exhibited smaller average grain diameters than their oxygen plasma treated (b,d,f) counterparts. All scan heights have been plotted from 0 to 60 nm.

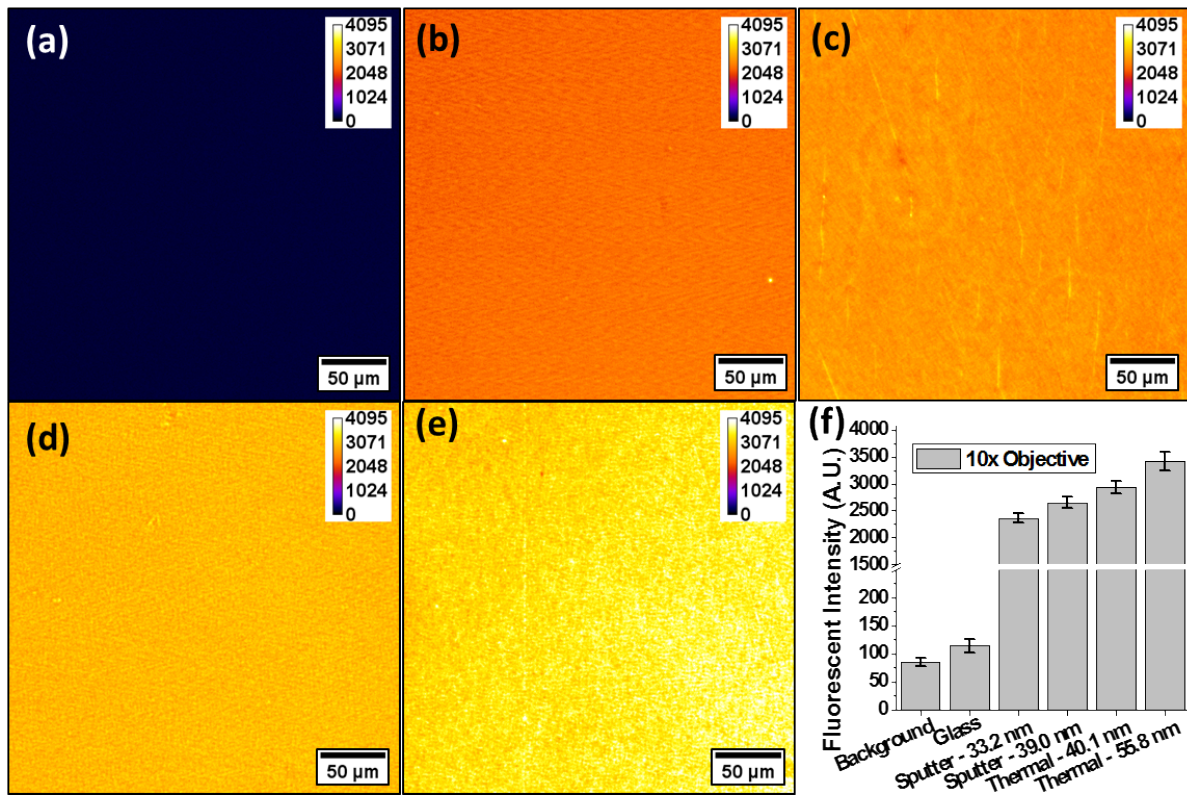


Fig. S2 Raw fluorescence images of (a) glass and silver gratings with a mean grain diameter of (b) 33.2 nm (sputtered Ti/Ag, no plasma), (c) 39.0 nm (sputtered Ti/Ag, plasma treated), (d) 40.1 nm (Thermal Cr/Ag, no plasma), and (e) 55.8 nm (Thermal Cr/Ag, plasma) samples with a 35 nm thick PMSSQ coating with 10 μ M Rhodamine 6G. All images were taken with a 10x objective, R6G filter cube, and 20 ms CCD exposure time. Images were false colored and scale bars were added to the image with open-source software (ImageJ). (f) Mean fluorescent intensity for all images including the background intensity of a glass sample without a dye layer.

Table S1. Summary of SPR peak location and parameters at $\theta_{\text{SPR}} = 15^\circ$ for silver gratings.

Surface Pre-treatment	Deposition Type	15° - ω SPR wavelength [nm]	Coupling Strength, σ [%]	FWHM [nm]
No	RF Sputtered Ge/Ag	530	30.9	29.0
Oxygen Plasma	RF Sputtered Ge/Ag	529	35.4	25.3
No	RF Sputtered Ti/Ag	526	39.9	15.9
Oxygen Plasma	RF Sputtered Ti/Ag	530	49.2	18.9
No	Thermally Evaporated Cr/Ag	528	45.2	15.9
Oxygen Plasma	Thermally Evaporated Cr/Ag	529	84.9	9.4

Table S2. Summary of simulated SPR peak parameters at $\theta_{\text{SPR}} = 15^\circ$ for silver gratings with different grain sizes.

Grain size	Wavelength (λ_{SPR} , nm)	FWHM (nm)	Quality factor (Q , a.u.) ($\lambda_{\text{SPR}}/\text{FWHM}$)	Coupling strength ($ R_{\text{peak}} - R_{\text{baseline}} $) (σ , a.u.)	Gamma (σ/FWHM) (γ , 10^{-2})	Peak area (a.u.)
small	538	19.3	40.2	84.2%	6.25	20.6
large	536	12.7	42.2	85.0%	6.69	14.7

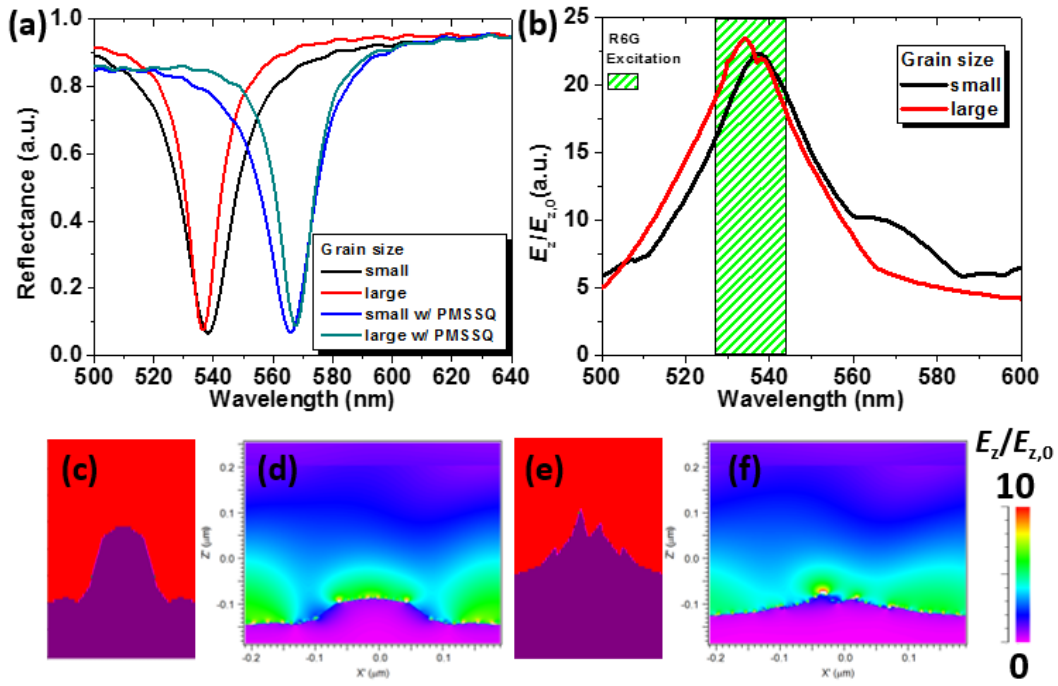


Fig. S3 (a) Simulated reflectivity plots for silver gratings with small and large grain sizes at 15° angle of TM-polarized incidence in air : with and without conformal PMSSQ coating. (b) maximum electric field ($E_z/E_{z,0}$) vs wavelength plots for silver gratings. Simulated profiles for (c) small grain size and (e) large grain size, the red region is air and the magenta region is silver and R6G excitation ranges. Electric field distribution under the wavelengths at reflectivity dips for (d) small grain size (538 nm) and (f) large grain size (536 nm), maximum $E_z/E_{z,0}$ is normalized at 10.

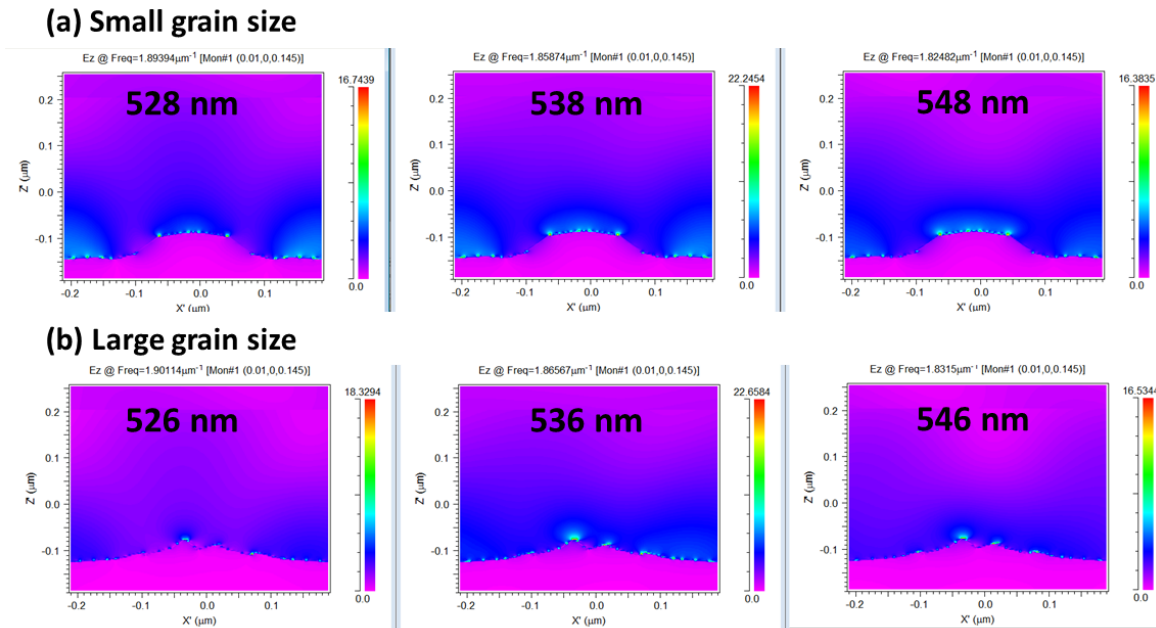
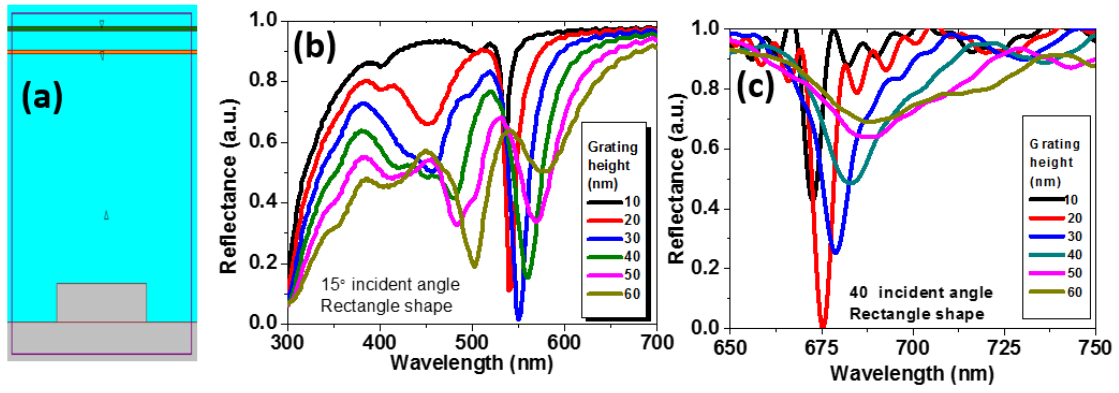
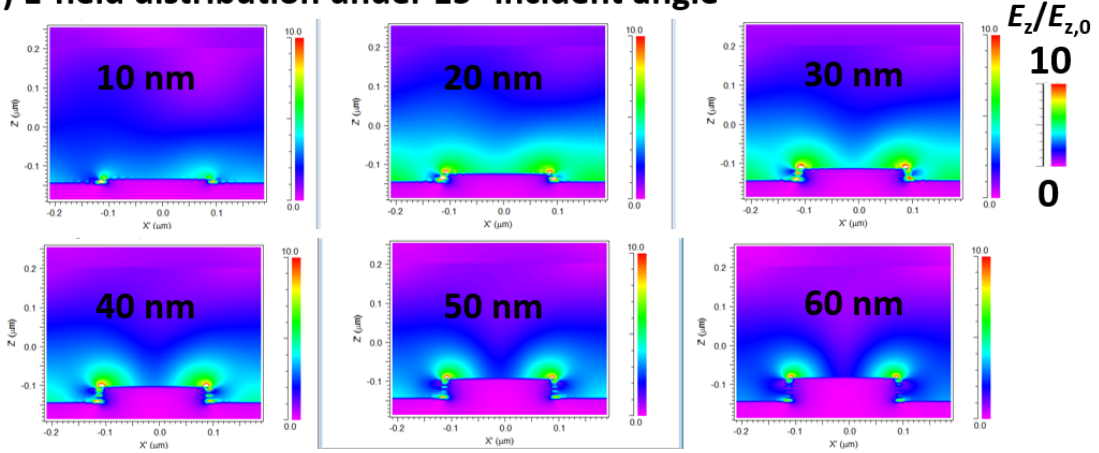


Fig. S4 Simulated electric field distribution ($E_z/E_{z,0}$) for silver gratings with small and large grain sizes at 15° angle of TM-polarized incidence in air under the wavelengths at reflectivity dips and 10 nm less or more than the SPR wavelength: (a) small grain size and (b) large grain size.



(d) E-field distribution under 15° incident angle



(e) E-field distribution under 40° incident angle

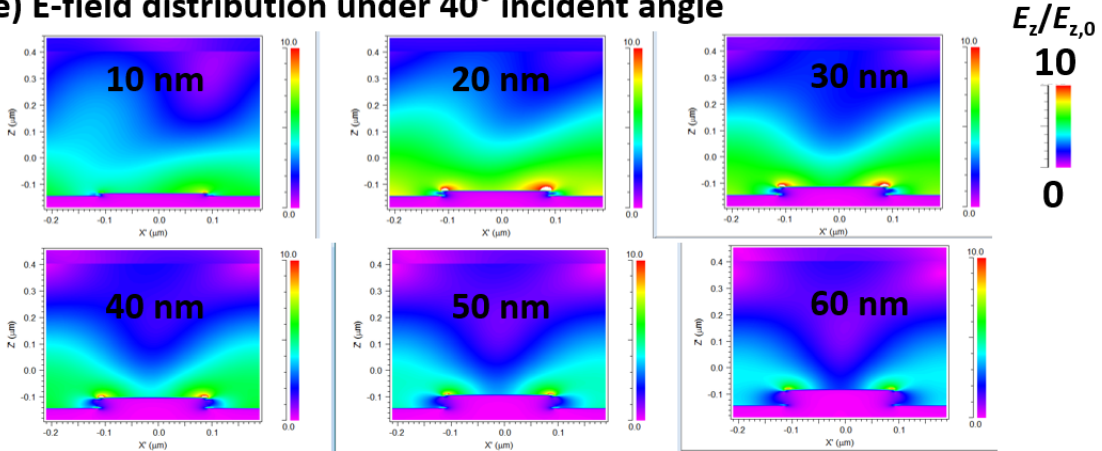


Fig. S5 (a) 2D simulation window for Ag gratings with rectangular shape varying grating heights from 10 nm to 60 nm. Simulated (b,c) reflectivity and (d,e) electric field distribution ($E_z/E_{z,0}$) for silver gratings with 0.5 of duty cycle at (b, d) 15° and (c, e) 40° angle of TM-polarized incidence in air under the wavelengths at reflectivity dips, maximum $E_z/E_{z,0}$ in scale bar is normalized at 10.

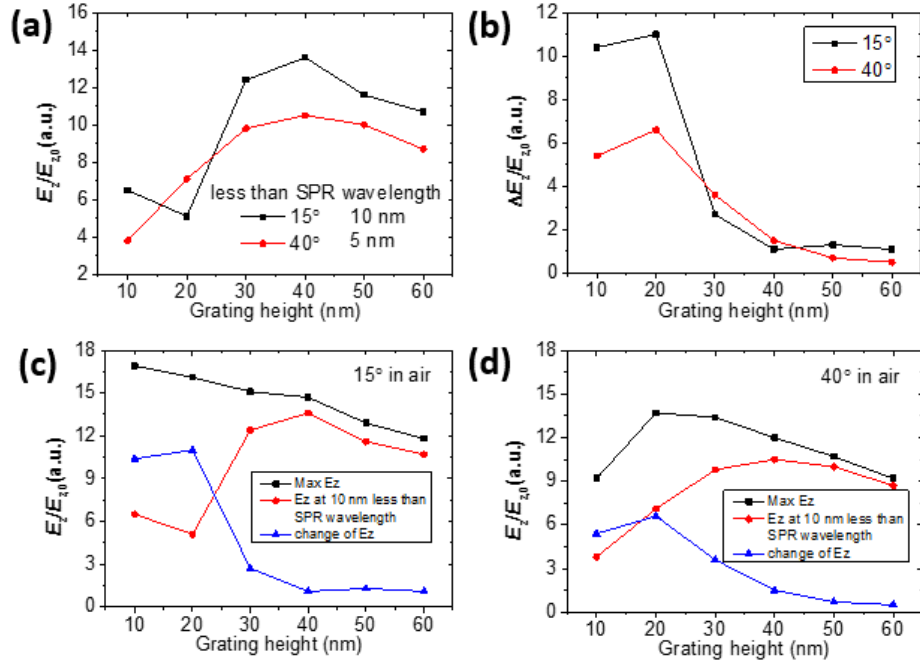


Fig. S6 Simulated SPR peak parameters at $\theta_{\text{SPR}} = 15^\circ$ and 40° for silver gratings with different grating heights, with constant duty cycle of 0.5: (a) electrical field at the wavelength (10 nm for 15° and 5 nm for 40°) less than SPR wavelength; (b) change of electrical field from between these wavelengths and SPR wavelengths. Electric field plots for (c) 15° and (d) 40° .

Table S3. Summary of simulated SPR peak parameters at $\theta_{\text{SPR}} = 15^\circ$ and 40° for silver gratings with different grating heights, with constant duty cycle of 0.5.

Grating height (nm)	SPR Wavelength (nm)		Max Ez		Ez (less than SPR wavelength)		Ez (change)	
	15°	40°	15°	40°	15°	40°	15°	40°
10	536	672.5	16.9	9.2	6.5	3.8	10.4	5.4
20	540	675.5	16.1	13.7	5.1	7.1	11	6.6
30	550	679	15.1	13.4	12.4	9.8	2.7	3.6
40	560	683	14.7	12	13.6	10.5	1.1	1.5
50	568	687.5	12.9	10.7	11.6	10	1.3	0.7
60	578	688	11.8	9.2	10.7	8.7	1.1	0.5

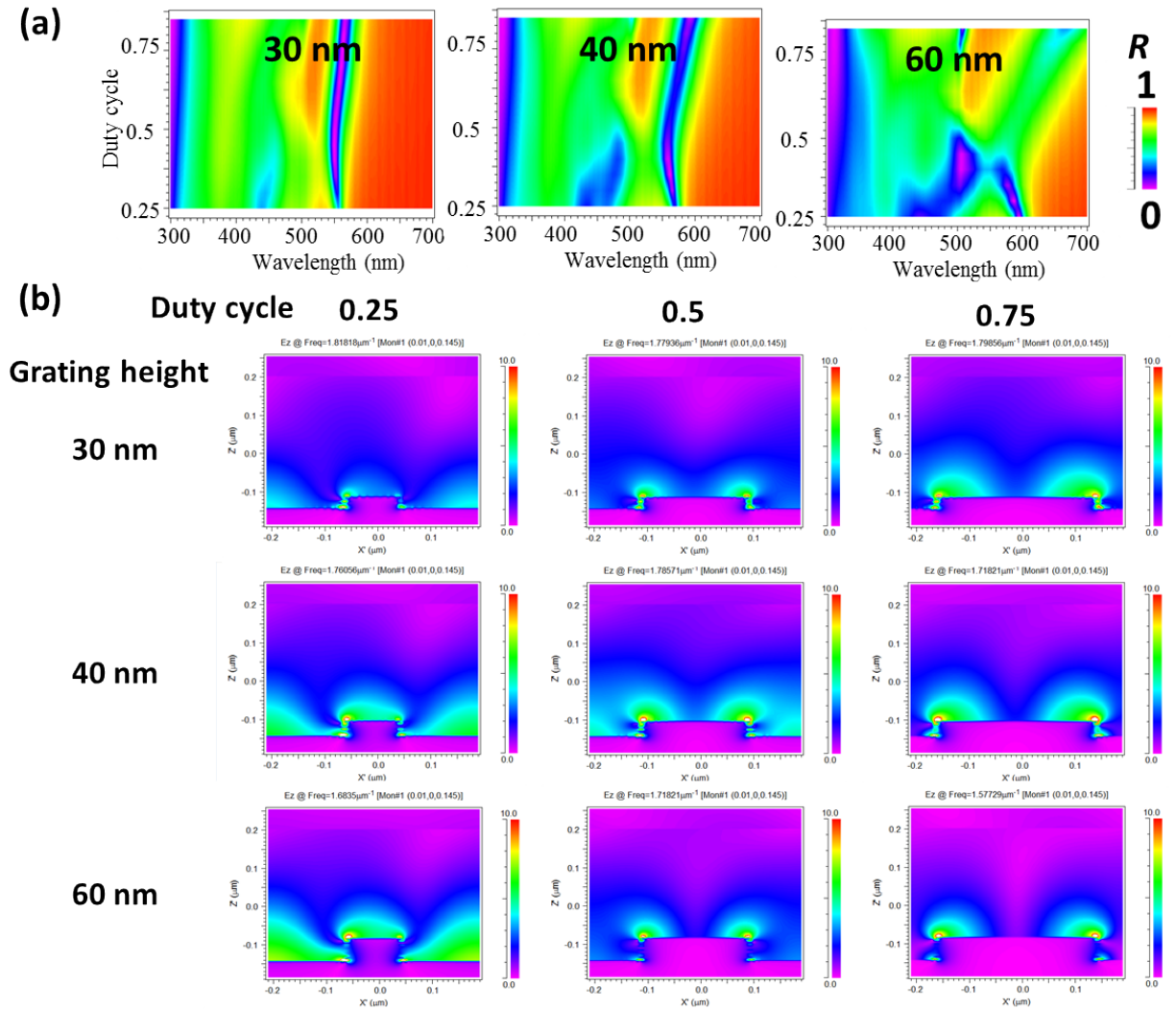


Fig. S7 (a) Reflectance (R) vs wavelength for varying grating duty cycles from 0.25 to 0.85 with constant grating height of 30 nm, 40 nm or 60 nm under each condition. (b) Electric field distribution ($E_z/E_{z,0}$) for silver gratings with varying duty cycle from 0.25 to 0.75 with grating heights of 30 nm, 40 nm and 60 nm, at 15° angle of TM-polarized incidence in air under the wavelengths at reflectivity dips, maximum $E_z/E_{z,0}$ in scale bar is normalized at 10.